Geotech Geol Eng (2024) 42:2259–2270
https://doi.org/10.1007/s10706-023-02672-6

ORIGINAL PAPER

Effect of Confining Pressure Unloading Rate on Mechanical and Energy Characteristics of Coal-Rock Combinations

Yuanjie Wang · Fabing Chen · Yan Li · Xuebo Sun · Ning Liu

Received: 20 July 2023 / Accepted: 30 September 2023 / Published online: 1 November 2023

Abstract Coal-rock combinations is a composite structure often encountered in mining engineering. At present, the research on coal-rock combinations mainly focuses on the loading mechanical properties. However, when mining engineering involves excavation, the mechanical characteristics of the coal-rock combination during unloading are very different from those during loading. In order to clarify the acoustic emission (AE) and energy evolution characteristics of unloading failure of coal-rock combinations, the numerical simulation of confining pressure unloading of coal-rock combinations under different unloading rates was carried out by using particle flow numerical simulation software. The mechanical characteristics of the failure process of the coal-rock combinations under different unloading rates were analyzed. The research results indicate that: With the increase of unloading rate, the number of AE events in coal-rock combination increases, the total number of cracks increases correspondingly, and the failure becomes more and more serious. The higher the unloading rate, the simpler the failure mode of the coal-rock combination, and the smaller the breaking angle. And the elastic strain energy, dissipation energy and total input energy of the coal-rock combination under different confining pressure unloading rates all increase with the increase of the unloading rate. However, the increases of the three are different, and the dissipation energy increases the most. The study can provide a reference for the unloading mechanical properties of the combination formed by coal and rock, and provides a reference for the excavation unloading speed when the half-coal and half-rock roadway is excavated.

Keywords Coal-rock combination · Unloading rates · Acoustic emission · Energy characteristics · Roadway excavation

Y. Wang · F. Chen (✉) · Y. Li · X. Sun · N. Liu
CCTEG Coal Mining Research Institute, Beijing 100013, China
e-mail: qingma819@hotmail.com

Y. Wang · F. Chen · Y. Li · X. Sun · N. Liu
Tiandi Science and Technology Co., Ltd, Beijing 100013, China

1 Introduction

Coal-rock combination is a combination structure often encountered in mining engineering. For example, the combination of coal pillars and roof or floor strata, the combination of coal and rock roadways in half-coal and half-rock roadways, the combination of coal seams and roof and floor strata during excavation, etc. (Tan et al. 2022; Pan et al. 2021; Ma et al. 2020). Roof and floor strata and coal seams or coal pillars constitute a composite load-bearing system, and the instability of any one of them will cause the overall failure. The composite structure composed of roof and floor rock strata and coal seams or coal

pillars is the main carrier of mining engineering (Gao et al. 2023; Li et al. 2022a, 2022b). Its overall stability and mechanical behavior have an important impact on the stability of the mine structure and mine safety.

At present, most of the studies on the mechanical behavior of surrounding rocks are concentrated on coal and rock alone, and the research on the overall mechanical behavior of coal-rock combination is also mainly focused on its loading mechanical characteristics. For example, Chen et al. (2023) studied the mechanical properties and damage characteristics of coal-rock combination under the action of water and rock. The deterioration mechanism of coal-rock combination under the action of water and rock is analyzed. And using the damage theory to build a damage model based on the water immersion time. Wu et al. (2023) studied the dip angle effect of the stress transfer and strength characteristics of the coal-rock combination, and obtained that the strength of the coal-rock combination decreases with the increase of the dip angle, which has certain theoretical reference significance for the safe and efficient mining of high-dip coal seams. Zuo and Song (2022) analyzed the evolution law of elastic energy density of coal mass and rock mass in coal-rock combinations. And from the viewpoint of non-equilibrium thermodynamics and dissipative structure, based on the analysis of coal-rock elastic energy density difference, the differential energy instability analysis model of combined coal-rock system is constructed. Yang et al. (2022) carried out the true triaxial single-plane air test of the coal-rock combination under the coupled action of high static load and dynamic and static load, and analyzed the mechanical characteristics and strength conditions at the interface of the coal-rock combination. The failure form, dynamic performance characteristics and evolution law of acoustic emission signals of coal-rock combination under different stress boundaries are explored. Yang et al. (2020) studied the mechanical response characteristics and energy partition evolution laws of coal rocks with different strength ratio combinations through laboratory uniaxial compression tests and numerical simulation calculations. Li et al. (2019) used the separate Hopkinson pressure bar (SHPB) to conduct impact compression tests on the prefabricated fractured coal-rock combination. The energy evolution characteristics of different fracture form combinations were explored. And the influence of crack position and inclination angle on the fracture fractal dimension of the combination is analyzed. Based on AE, digital camera video and SEM system, Yin et al. (2018) conducted uniaxial compression tests on roof sandstone-coal pillar structure samples under different loading rates. The effect of loading rate on the mechanical behavior of the roof-coal pillar structure was studied. In addition, some scholars have studied the influence of factors such as coal-rock height ratio, coal-rock interface dip angle, and coal-rock interface parameters on the mechanical properties of coal-rock combinations. At the same time, acoustic and electrophysical signal characteristics such as acoustic emission characteristics and electromagnetic radiation characteristics of the coal-rock combination were analyzed (Hu et al. 2023; Duan et al. 2023; Dong et al. 2020). The above research has played a very good guiding role in the stability analysis of coal-rock combination. However, most of the current studies on the mechanical properties of composites focus on the loading mechanical properties, and there is a lack of research on the unloading mechanical properties of coal-rock combinations. The stress unloading caused by roadway excavation and coal seam mining will change the stress state of the original rock. The rock mass will be deformed and destroyed in the direction of unloading, and the mechanical properties of coal and rock will be changed accordingly. It may cause disasters and accidents such as rock burst, water inrush, gas outburst, carbon dioxide and nuclear waste overflow, and pose a serious threat to engineering production and safety.

Based on this, this paper takes the excavation of half-coal and half-rock roadway under unstable stratum conditions as the engineering background, and studies the unloading mechanical characteristics of coal-rock combination through numerical simulation software. At the same time, the influence of the unloading rate on the mechanical and acoustic emission characteristics of the coal-rock combination is analyzed. In addition, the influence of the unloading rate on the energy characteristics of the coal-rock combination is also obtained by using the energy calculation method. The research of this paper aims to provide reference for the excavation and unloading speed during the excavation of half-coal and half-rock roadway.

2 Engineering Background

In some mining areas, due to the extremely unstable strata, the roadways are often arranged in the coal seam, forming a half-coal and half-rock roadway layout method (Yu et al. 2014; Yang et al. 2016; Shabanimashcool and Li 2013; Singh et al. 2011), As shown in Fig. 1. When this type of roadway is excavated, the stability of the roadway is not only related to the mechanical properties of coal or rock. It is also closely related to the mechanical properties of the combination whole formed by coal rock. The essence of the excavation problem in rock underground engineering and roadway excavation is that the stress or strain of the rock mass in a certain direction is released, thereby destroying the original mechanical balance state, causing new deformations, even fractures, and fragments of the rock mass. The excavation and unloading of the half-coal and half-rock roadway will also have a certain impact on the coal-rock combination, and the mechanical properties will change greatly at different excavation and unloading speeds. Roadway instability is the result of the overall failure of coal-rock combination, and the excavation unloading speed is also crucial to its stability during the excavation process (Peng and Liu 2020; Wang and Xie 2010; Zhang et al. 2017; Son and Moon 2017; Wang et al. 2020).

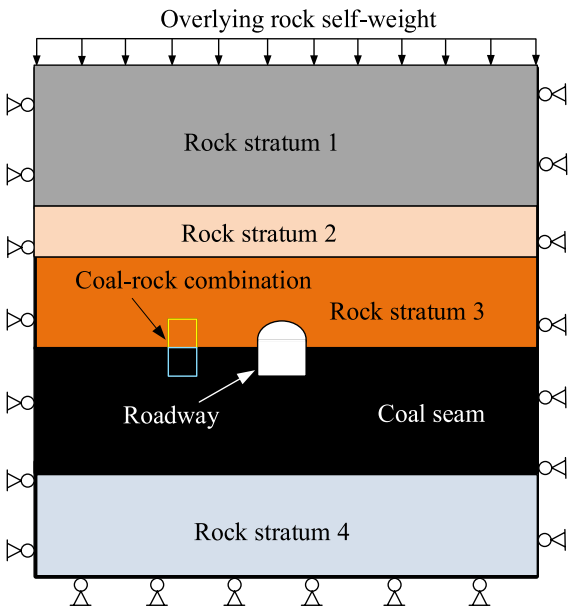

Fig. 1 Schematic diagram of roadway excavated in half coal and half rock

The mechanical behavior of rock under excavation and mining conditions can be simply obtained from routine laboratory tests or numerical simulation test curves. Although there will be certain errors, they will reflect the same laws. Next, the numerical simulation test will be carried out on the standard rock mechanics test specimen ($d \times h = 50 \times 100$ mm) of the coal-rock combination through the numerical simulation software PFC, and the influence of the unloading rate on its mechanical, AE and energy characteristics will be studied.

3 Numerical Computational Model

3.1 Numerical Model

Cundall and Strack (1983) introduces the particle flow theory created by molecular dynamics, focusing on analyzing the damage characteristics of materials from the perspective of mesomechanics. It enables the study of large deformation processes from linear elasticity up to failure. It is mainly used in the study of rock materials without defining the constitutive model of the material. Only need to set the mesomechanical parameters and the bonding model between particles, the complex nonlinear stress–strain relationship can be expressed. The parallel bond model (Linearpbond) in the PFC program can transmit force and moment between different entities, and can also resist shear and tension caused by external forces (Cundall and Strack 1983). Therefore, in this paper, the Linearpbond model is used to simulate the unloading mechanical properties of coal-rock combination. The constitutive behavior of the microscopic parameters in the parallel bond model is shown in Fig. 2.

In this paper, the particle flow software PFC is used to establish the coal-rock combination model. First, a numerical test container of a standard rock sample model with a size of 50 mm × 100 mm is generated. Then, by adding a joint surface with the JSET command in the middle of the model, the model is divided into upper and lower parts, which are used to simulate rock and coal respectively. Then determine the mesoscopic parameters of the model. In the Linearpbond model, the mesoscopic parameters mainly include parallel bond modulus, parallel bond stiffness

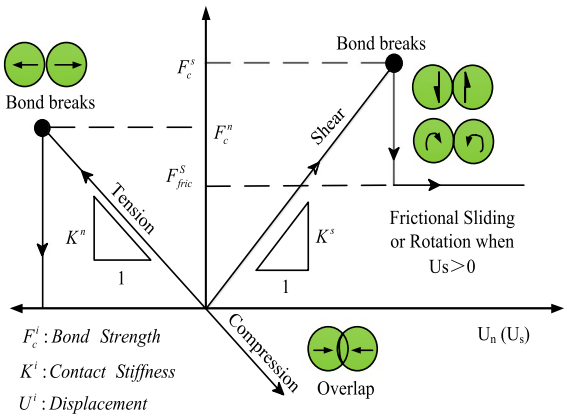

Fig. 2 Constitutive behavior of microcosmic parameters in PFC simulation (Cundall and Strack 1983)

ratio, normal bond strength, tangential bond strength, etc. Reference (Guo et al. 2018) has already checked the mesoscopic parameters, so for convenience, this simulation selects the coal and rock mesoscopic parameters in the literature (Guo et al. 2018), as listed in Table 1. The established coal-rock combination model is shown in Fig. 3. A total of 21,390 round particles of different scales were generated. Among them, the minimum particle radius is 0.2 mm, and the maximum particle radius is 0.3 mm.

3.2 Numerical Simulation Scheme

In order to determine the strength and deformation characteristics of the coal-rock combination under different confining pressure unloading rates, the conventional biaxial compression test of the coal-rock combinations under the confining pressure of 5 MPa is firstly carried out. The strength value of the coal-rock combinations under the confining pressure of 5 MPa under conventional biaxial loading is obtained. Then the confining pressure unloading test of the coal-rock combinations under different unloading rates is carried out. The unloading test procedure is to first increase the confining pressure at a loading rate of 0.05 mm/s to the set confining pressure of 5 MPa. Then add axial compression at a rate of 0.05 mm/s to 50% of the axial compression strength when the confining pressure of conventional biaxial loading is

Table 1 Micromechanical parameters of coal and rock (Guo et al. 2018)

Mechanical parameters	ρ/kg m^{-3}	R_{min}/mm	R_{max}/R_{min}	*Ec*/GPa	*Kn/Ks*	$\overline{E}$/GPa	$\overline{K}_n/\overline{K}_s$	$\overline{\sigma}_c$/MPa	$\overline{\tau}_c$/MPa	μ
Rock	2600	0.2	1.5	12	2.5	12	2.5	45	45	0.5
Coal	1800	0.2	1.5	4	2.5	4	2.5	15	15	0.5

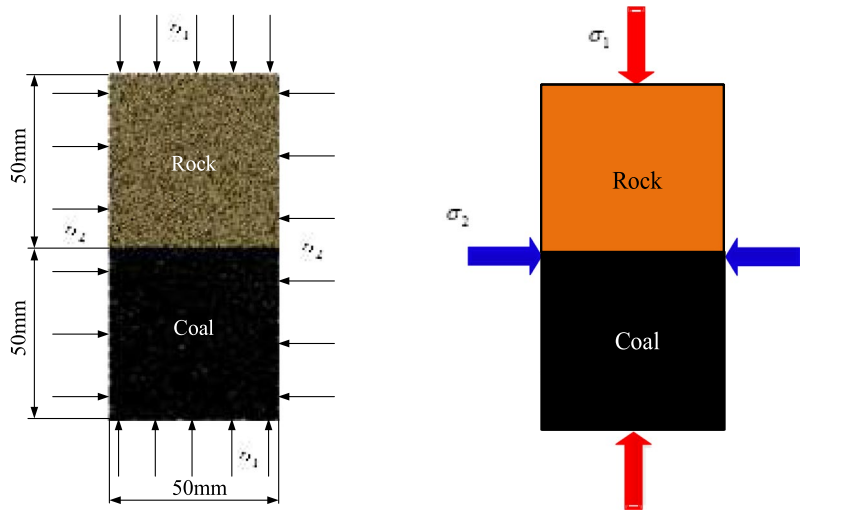

Fig. 3 Numerical calculation model and physical model of coal-rock combination samples

(a) Numerical model of coal-rock combination (b) Physical model of coal-rock combination

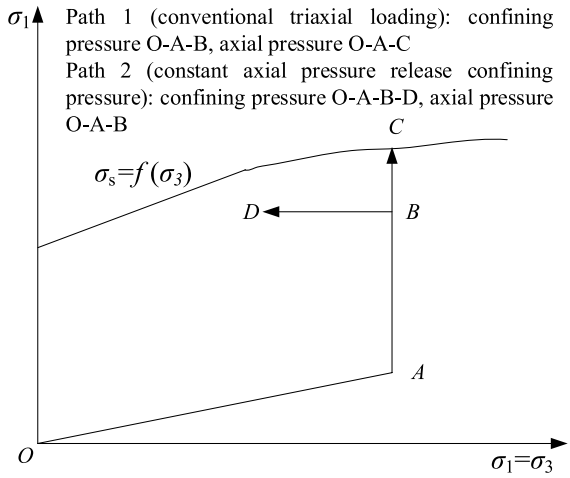

Fig. 4 Schematic diagram of stress path changes during the test

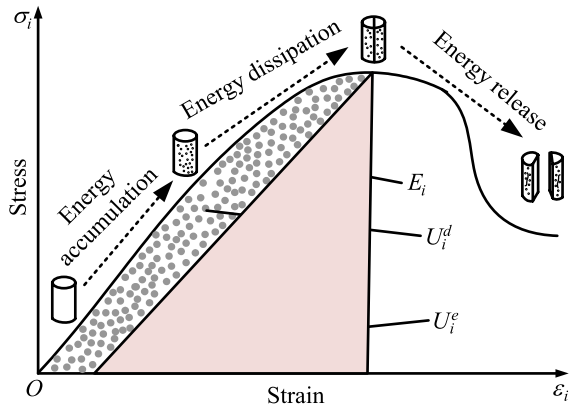

Fig. 5 Relationship between dissipative energy and releasable strain energy of coal and rock (Xie et al. 2005; Ma et al. 2021; Zhou et al. 2023)

5 MPa. Then keep the axial pressure constant, and release the confining pressure at the rate of 0.001, 0.005, 0.01, 0.025 and 0.05 mm/s respectively. Stop the simulation test until the sample is destroyed. The conventional biaxial loading and unloading paths are shown in Fig. 4.

3.3 Energy Calculation Method

The energy change in the coal-rock combination during loading and unloading is shown in Fig. 5. The calculation method of the total input energy U, dissipation energy U_d, and elastic strain energy U_e of the coal-rock combination at different unloading rates refers to the calculation method of Xie et al. (Xie et al. 2005; Ma et al. 2021; Zhou et al. 2023), as follows

$$U = \int_0^{\varepsilon_1} \sigma_1 d\varepsilon_1 + \int_0^{\varepsilon_2} \sigma_2 d\varepsilon_2 + \int_0^{\varepsilon_3} \sigma_3 d\varepsilon_3 \quad (1)$$

$$U^e = \frac{1}{2\bar{E}}\left[\sigma_1^2 + \sigma_2^2 + \sigma_3^2 - 2\bar{\nu}\left(\sigma_1\sigma_2 + \sigma_2\sigma_3 + \sigma_1\sigma_3\right)\right] \quad (2)$$

$$U = U_e + U_d \quad (3)$$

where $\overline{E}$ and $\overline{\nu}$ are the average values of the unloading elastic modulus and Poisson's ratio, respectively. U, U_d, and U_e are the total input energy, dissipation energy and elastic strain energy, respectively. ε_i is the Total strain in direction of main stress σ_i.

4 Results and Discussion

4.1 AE Characteristics of Coal-Rock Combination at Different Rates of Unloading Confining Pressure

In PFC2D BPM, each crack formation forms an AE pulse (Ma et al. 2020; Zhao et al. 2016; Du et al. 2018; Zhang et al. 2023). There are also differences in the AE characteristics and generation mechanism of the coal-rock combination sample under the effect of different confining pressure unloading rate. By recording number of cracks and the post-processing of data during uniaxial compression of coal-rock combination with different unloading rates, calculation of AE events for the failure of coal-rock combination can be simulated. And the effect of different confining pressure unloading rate on AE characteristics of coal-rock combination samples will be obtained. Figure 6 is a counting diagram of AE events at different unloading rates for the coal-rock combination under the same confining pressure. It can be seen from the figure that the whole failure process of the coal-rock combination under the same confining pressure and different confining pressure unloading rates can be divided into five stages for analysis. (1) Steady stage of AE: The coal-rock combination has passed the compaction stage, and at the beginning

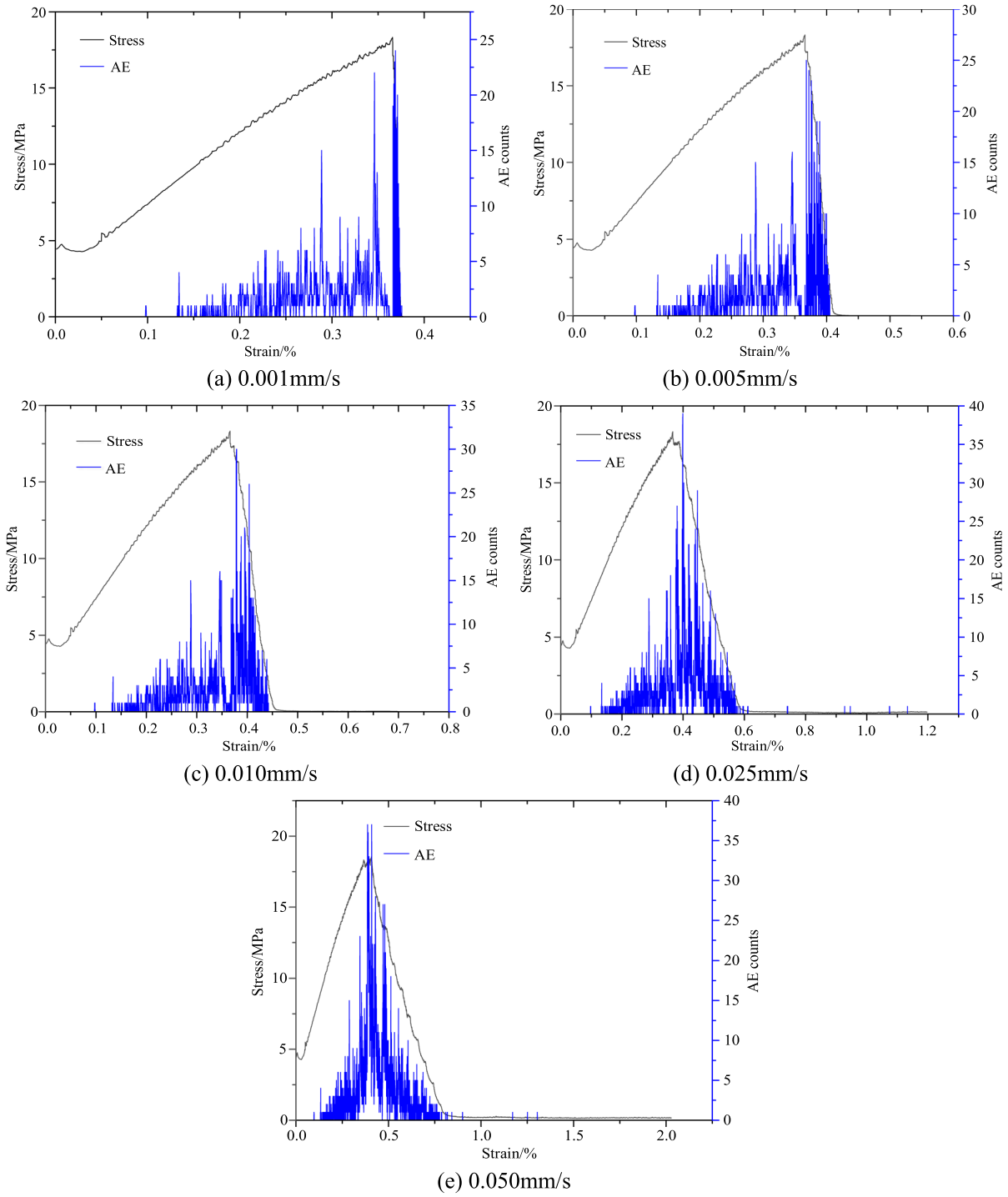

Fig. 6 AE events of coal-rock combination under different unloading rates

of unloading, the disturbance is relatively small, and the acoustic emission event count is at a very low level. (2) The initial increase stage of AE: As the unloading continues, the stress difference between the axial pressure and the confining pressure continues to increase, and at this stage the coal-rock combination produces a small amount of acoustic emission signal and the signal is getting stronger. (3) AE unstable stage: Unsteady changes in AE event counts as the stress difference continues to increase. (4) AE burst stage: The confining pressure is continuously unloaded, the stress difference reaches the maximum, the number of AE events reaches the maximum, and the coal-rock combination is destroyed with the continuous unloading of the confining pressure. (5) AE disappear stage: After the unloading is over, the AE signal of the assembly destruction disappears. Regardless of the unloading rate, the AE event count during the unloading process basically changes in these five stages. Therefore, stage (3), the initial unstable stage of AE, can be regarded as the precursor signal of unloading damage.

The difference is that with the increase of the unloading rate of the confining pressure, the number of AE events during the unloading failure of the coal-rock combination increases continuously. When the unloading rate increased from 0.001 to 0.050 mm/s, the count of AE events increased from 24 to 39, an increase rate of 63%. That is, the greater the unloading rate, the more serious the damage of the coal-rock combination will be. It can also be seen from the figure that the faster the unloading rate of the confining pressure is, the faster the confining pressure decreases, the shorter the time required for the destruction process of the coal-rock combination, and the more severe the damage is.

4.2 Crack Number Change and Deformation Failure Characteristics of Coal-Rock Combination with Different Confining Pressure Unloading Rates

Figure 7 is the change diagram of the number of cracks in the coal-rock combination under different unloading rates. It can be seen from Fig. 7 that at different unloading rates, the number of cracks in the coal-rock combination has the same trend. That is, the number of cracks basically does not change at the beginning of unloading. With the progress of unloading, the stress difference between axial pressure and confining pressure increases, and the number of cracks increases slowly. Then when approaching unloading failure point, the number of cracks increased rapidly, and the combination sample was damaged. Then the number of cracks does not change after unloading. The difference is that as the unloading rate increases, the total number of cracks increases correspondingly. From 4504 when the unloading rate is 0.001 mm/s to 6125 when the unloading rate is 0.05 mm/s, with an increase of 36%.

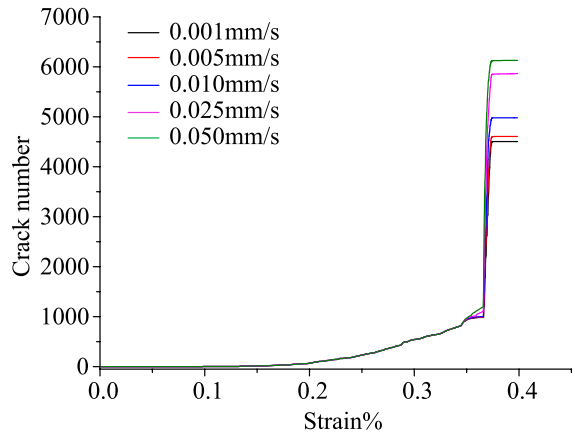

Fig. 7 Changes in the number of cracks in the coal-rock combination under different unloading rates

The failure modes of coal-rock combination at different confining pressure unloading rates. It can be seen from Fig. 8:

(1) The unloading failure surface of the coal-rock combination is mainly the combined failure of shear and tension. With the increase of the unloading rate, the surface of the coal-rock combination gradually changes from composite tensile shear failure to shear failure.
(2) The higher the unloading rate, the simpler the failure mode of the coal-rock combination. And the breaking angle has a decreasing trend. This is because the greater the unloading rate, the closer the coal-rock composite sample is to the uniaxial compression state.
(3) When the unloading rate is small, the damage of the coal-rock combination mainly occurs in the coal mass. With the increase of the unloading rate, the failure of the coal-rock combination not only occurs in the coal body part, but also in the

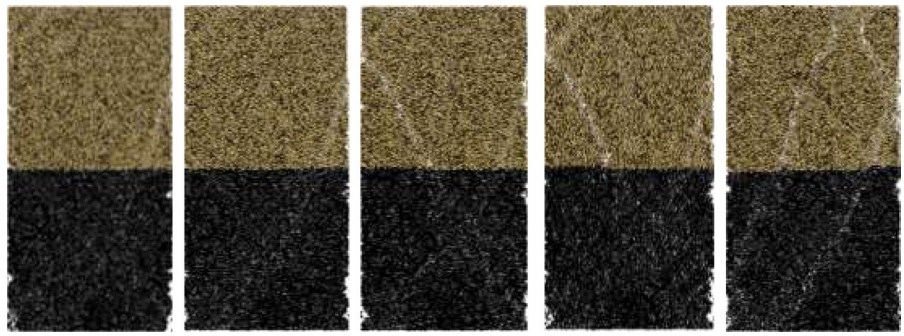

Fig. 8 Failure diagrams of coal-rock combination at different unloading rates

rock part. And the greater the unloading rate, the more serious the damage of the rock part.

The unloading of confining pressure has a significant impact on the strength of coal-rock combined body. After unloading, the cohesion and internal friction angle of the coal-rock combined body are significantly reduced (Chen and Li 2008). The process of coal-rock combined body damage and failure under unloading confining pressure is the transition of coal-rock combined body from a high confining pressure stress state to a low confining pressure state. That is, the transition from a plastic state to a brittle state. Compared to continuous loading failure, unloading failure is more sudden, similar to splitting failure under uniaxial compression.

4.3 Energy Characteristics of Coal-Rock Combination with Different Confining Pressure Unloading Rates

Figure 9 shows the energy evolution curves of coal-rock combination under different confining pressure unloading rates. It can be seen from Fig. 9 that the elastic strain energy, dissipated energy and total input energy of coal-rock combination under different unloading rates are basically the same. Before the unloading failure point, the three factors increase continuously with the increase of strain. Initially the rate of increase of elastic strain energy is lower than the rate of increase of dissipated energy. The increase rate of elastic strain energy increases rapidly when approaching the unloading failure point. When the stress peak value is reached, the elastic energy storage reaches a certain surface energy of the specimen unit. A large amount of elastic energy is released quickly, and the cracks of the coal-rock composite sample converge and penetrate, forming a macroscopic fracture surface. Failure occurs in a very short time. Dissipated energy rises rapidly. Compared with the degree of energy conversion before the peak stress, the energy conversion at this stage is more intense. After entering the plastic flow stage, the axial strain continues to increase with time, but the energy change tends to be moderate. All energies are basically stable, or the amount of change is small.

In order to more intuitively compare the influence of unloading rate on the elastic strain energy and dissipation energy of coal-rock combinations, the curves of elastic strain energy, dissipation energy and total input energy at the peak strength of coal-rock combinations under different unloading rates are drawn (Fig. 10). It can be seen from Fig. 10 that the elastic strain energy, dissipation energy and total input energy at the peak strength of the coal-rock combinations at different unloading rates all increase with the increase of the unloading rate. However, the increases of the three are different. When the unloading rate increases from 0.001 to 0.050 mm/s, the increase rates of elastic strain energy, dissipation energy and total input energy are 15.90%, 67.03%, and 39.78% respectively.

5 Discussion

The problem of rock mass unloading failure caused by underground engineering such as tunnel excavation has attracted attention in the field of rock mechanics due to its different failure mechanisms from those under continuous loading. In mining engineering, a large number of coal pillars have

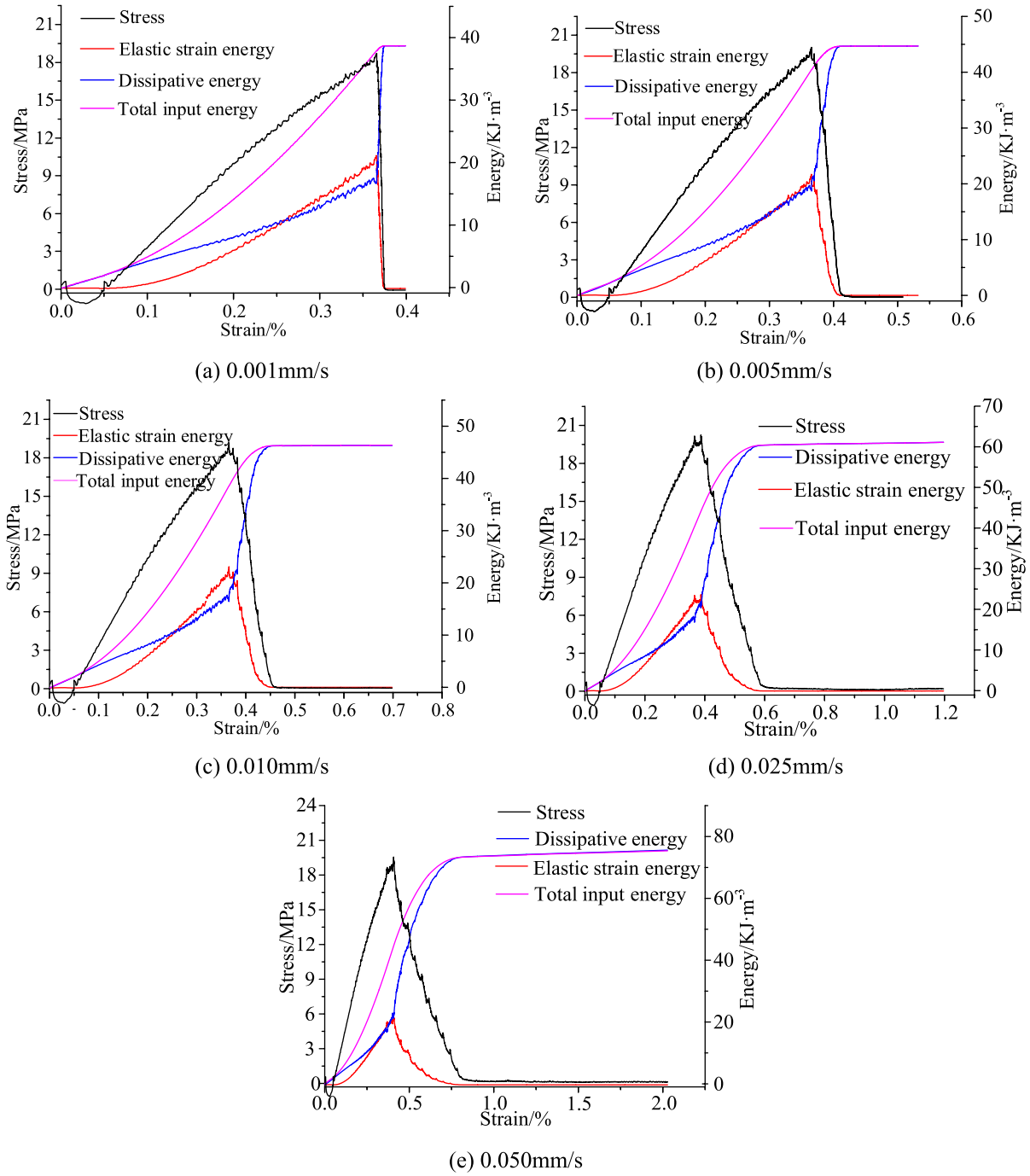

Fig. 9 Energy evolution characteristics of coal-rock combination under different unloading rates

been left for safety, protection, waterproofing, and other purposes. The coal pillars form a combination of coal and rock with the roof and floor rocks. Numerous studies have been conducted on the loading mechanical properties of coal-rock combined body, but little has been done on the unloading mechanical properties of coal-rock combined body. Based on this, this article studies the effect

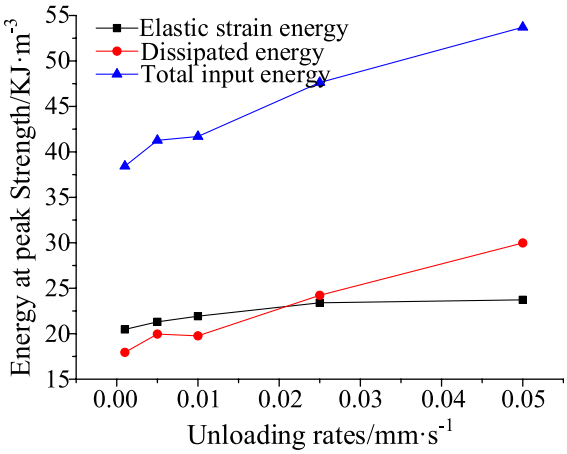

Fig. 10 Variation curves of elastic strain energy, dissipation energy and total input energy at the peak strength of coal-rock combination under different unloading rates

of confining pressure unloading rate on mechanical and energy characteristics of coal-rock combinations. The AE, changes in the number of microcracks, and energy characteristics of coal-rock combinations under different unloading rates were obtained. The results show that the unloading of confining pressure has a significant impact on the strength of coal-rock combined body. After unloading, the cohesion and internal friction angle of the coal-rock combined body are significantly reduced. The process of coal-rock combined body damage and failure under unloading confining pressure is the transition of coal-rock combined body from a high confining pressure stress state to a low confining pressure state. That is, the transition from a plastic state to a brittle state. Compared to continuous loading failure, unloading failure is more sudden, similar to splitting failure under uniaxial compression.

However, the paper did not compare the differences in loading and unloading mechanical properties of coal-rock combinations. There is also no comparison of the mechanical properties of coal, rock monomer, and coal-rock combination under unloading conditions. Although literature (Ma et al. 2021) has studied the characteristics of coal-rock combinations under different loading rates (Fig. 11), the rate is different from the unloading rate in this paper.

However, from Fig. 11, it can be seen that the failure form of the coal-rock combination during loading mainly occurs in the coal body part. The rock part of the coal-rock combination is basically not damaged. The failure of the coal-rock combination during unloading is more severe than that during loading. Compared to continuous loading failure, unloading failure is more sudden, similar to splitting failure under uniaxial compression. However, when comparing the mechanical characteristics of coal-rock combinations during loading and unloading, it is necessary to compare various mechanical characteristics at the same rate. At the same time, it is also necessary to conduct research on the comparison of coal, rock monomers, and coal-rock combinations under unloading action in our future work.

6 Conclusions

(1) The AE changes in the whole failure process of coal-rock combination at different unloading rates can be roughly divided into the following five stages: AE stable stage, AE initial increase stage, AE initial instability stage, AE burst stage, AE disappearance stage. With the increase of

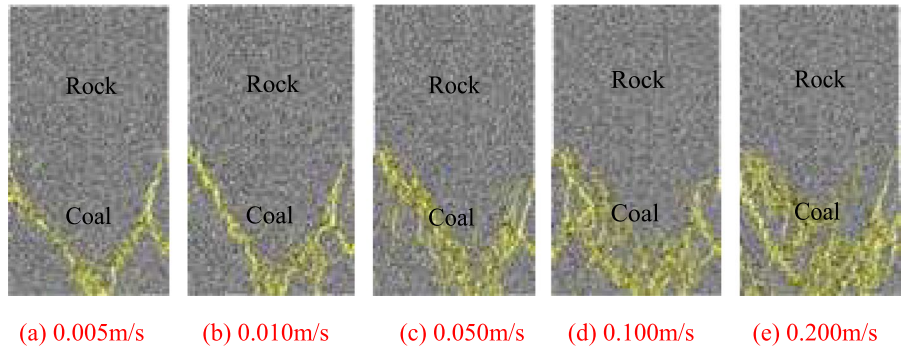

Fig. 11 Micro cracks at failure in the coal-rock composite samples under different loading rates (Ma et al. 2021)

unloading rate, the count of AE events during unloading failure of coal-rock combination is increasing. When the unloading rate increased from 0.001 to 0.050 mm/s, the number of AE events increased from 24 to 39, with an increase rate of 62.5%.

(2) The unloading failure forms of the coal-rock combinations is mainly the combined failure of shear and tension. With the increase of the unloading rate, the forms of the coal-rock combination gradually changes from composite tensile shear failure to shear failure. When the unloading rate is small, the damage of the coal-rock combination mainly occurs in the coal body part. With the increase of the unloading rate, the failure of the coal-rock combination not only occurs in the coal body part, but also in the rock part of the combination.

(3) The change trends of elastic strain energy, dissipation energy and total input energy of coal-rock combination under different unloading rates are basically the same. Before the unloading failure point, the three all increase with the increase of strain. The dissipated energy increases rapidly and the elastic strain energy decreases rapidly during unloading failure. At different unloading rates, the elastic strain energy, dissipation energy and total input energy at the failure point all increase with the increase of unloading rate. When the unloading rate increases from 0.001 to 0.050 mm/s, the increase rates of elastic strain energy, dissipation energy and total input energy are 15.90%, 67.03%, and 39.78%, respectively.

Although the study can provide a reference for the excavation unloading speed when the half-coal and half-rock roadway is excavated, it still has a few shortcomings. For instance, there is currently no comparison of the differences of mechanical characteristics between loading and unloading of coal-rock combination. There is also no comparison of the mechanical properties of coal, rock monomer, and coal-rock combination under unloading conditions. Last, further research is needed on the failure mechanism of coal-rock combinations under different unloading rates. Thus, we can take more targeted actions by researching the relationships and finding the connection among the various types of loading or unloading forms.

Funding This study was supported by the Major science and technology projects of China National Coal Group Corp (No. 20211BY001).

Data Availability Enquiries about data availability should be directed to the authors.

Declarations

Conflict of interest The authors declare they have no potential conflicts of interest with respect to the research, authorship, and/or publication of this article.

References

Chen XT, Li L (2008) Experimental study of unloading mechanic properties of rock under high confining pressure and high water pressure. Chin J Rock Mech Eng 27:2694–2699

Chen GB, Li T, Yang L, Zhang GH, Lv PF, Teng PC (2023) Mechanical properties and damage characteristics of coal-rock combined samples under water-rock interaction. Coal Sci Technol 51(4):37–46

Cundall PA, Strack O (1983) Modeling of microscopic mechanisms in granular material. Stud Appl Mech 7:137–149

Dong SN, Li A, Ji YD, Yang YX, Mu Q (2020) Mechanical and failure characteristics of rock-coal-rock combined body under different strain rates: a numerical study from micro perspective. Geotech Geol Eng 39:185–191

Du F, Wang K, Wang GD, Jiang YF, Xin CP, Zhang X (2018) Investigation on acoustic emission characteristics during deformation and failure of gas-bearing coal-rock combined bodies. J Loss Prev Process Ind 55:253–266

Duan HQ, Xiong S, Yu WB (2023) Numerical simulation study on mechanical and acoustic emission characteristics of coal-rock combined body subjected to cyclic disturbing loading. Geotech Geol Eng 41:783–802

Gao L, Shen Y, Liu P, Wang Y, Ma Z, Kang X (2023) Study on the coal-rock ratio effect of asymmetric deformation and failure of the gob-side coal-rock roadway in gently inclined coal seam. Geotech Geol Eng 41:243–255

Guo WY, Tan YL, Yu FH, Zhao TB, Hu SC, Huang DM, Qin ZW (2018) Mechanical behavior of rock-coal-rock specimens with different coal thicknesses. Geomech Eng 15(4):1017–1027

Hu SC, Zhou XD, Ru WK, Han JM, Guo SH, Zhang CX, Yang L (2023) Study on mechanical property of coal-rock combination under different unloading confining pressure rate. Geotech Geol Eng 41:2629–2644

Li CJ, Xu Y, Zhang YT, Li HL (2019) Study on energy evolution and fractal characteristics of cracked coal-rock-like combined body under impact loading. Chin J Rock Mech Eng 38(11):2231–2241

Li T, Chen GB, Li YH, Li QH (2022a) Study on progressive instability characteristics of coal-rock composite structure with the different height ratios. Geotech Geol Eng 40:1135–1148

Li T, Chen GB, Qin ZC, Li QH (2022b) Analysis the characteristic of energy and damage of coal-rock

composite structure under cycle loading. Geotech Geol Eng 40:765–783
Ma Q, Tan YL, Liu XS, Gu QH, Li XB (2020) Effect of coal thicknesses on energy evolution characteristics of roof rock-coal-floor rock sandwich composite structure and its damage constitutive model. Compos B Eng 198(1):108086
Ma Q, Tan YL, Liu XS, Zhao ZH, Fan DY, Purev L (2021) Experimental and numerical simulation of loading rate effects on failure and strain energy characteristics of coal-rock composite samples. J Cent South Univ 28(10):3207–3222
Pan B, Yu W, Shen W (2021) Experimental study on energy evolution and failure characteristics of rock-coal-rock combination with different height ratios. Geotech Geol Eng 39:425–435
Peng C, Liu W (2020) Analysis of stress removal effect of borehole depth and position on coal-rock with shock tendency. Geotech Geol Eng 38:4099–4109
Shabanimashcool M, Li CC (2013) A numerical study of stress changes in barrier pillars and a border area in a longwall coal mine. Int J Coal Geol 106:39–47
Singh R, Mandal PK, Singh AK, Kumar R, Sinha A (2011) Coal pillar extraction at deep cover: With special reference to Indian coalfields. Int J Coal Geol 86(2–3):276–288
Son M, Moon HK (2017) The hydraulic stability assessment of jointed rock mass by analysis of stress path due to underground excavation. KSCE J Civ Eng 21:2450–2458
Tan YL, Ma Q, Liu XS, Zhao ZH, Zhao MX, Li L (2022) Failure prediction from crack evolution and acoustic emission characteristics of coal-rock sandwich composite samples under uniaxial compression. Bull Eng Geol Env 81(5):1–15
Wang L, Xie GX (2010) Research on the influence of the advance speed of fully mechanized mining face on coal and rock dynamic disaster. J China Univ Min Technol 01:70–74
Wang E, Chen G, Yang X, Zhang G, Guo W (2020) Study on the failure mechanism for coal roadway stability in jointed rock mass due to the excavation unloading effect. Energies 13(10):2515
Wu YP, Yan ZZ, Luo SH, Tang YP, Wang T, Cao JL (2023) Dip effect of stress transfer and structural instability mechanism of coal-rock combination. Coal Sci Technol 51(1):12
Xie HP, Peng RD, Ju Y (2005) Zhou HW (2005) Oo energy analysis of rock failure. Chin J Rock Mech Eng 24(15):6
Yang SQ, Chen M, Jing HW, Chen KF, Meng B (2016) A case study on large deformation failure mechanism of deep soft rock roadway in Xin'An coal mine, China. Eng Geol 217:89–101
Yang L, Gao FQ, Wang XQ (2020) Mechanical response and energy partition evolution of coal-rock combinations with different strength ratios. Chin J Rock Mech Eng 39(2):3297–3305
Yang K, Liu WJ, Ma YK, Xu RJ, Chi XL (2022) Experimental study of impact failure characteristics of coal-rock combination bodies under true triaxial loading and single face unloading. Rock Soil Mech 43(1):15–27
Yin DW, Chen SJ, Xing WB, Huang DM, Liu XQ (2018) Experimental study on mechanical behavior of roof-coal pillar structure body under different loading rates. J China Coal Soc 43(05):1249–1257
Yu WJ, Feng T, Wang WJ, Liu H, Ma PY, Wang P, Li RH (2014) Deformation mechanism control principle and technology of soft half coal rock roadway. Chin J Rock Mech Eng 33(4):658–671
Zhang HW, Li YP, Chen Y, Zhu F, Shao LF (2017) Study on safety pushing forward speed of island coal mining face under hard roof and hard seam and hard floor conditions. Coal Sci Technol 045(2):6–11
Zhang Q, Zhou XP, Yang SQ (2023) Numerical study of fracture failure nature around the circular and horseshoe openings using the bonded-particle model. Geophys J Int 232:725–737
Zhao TB, Guo WY, Lu CP, Zhao GM (2016) Failure characteristics of combined coal-rock with different interfacial angles. Geomech Eng 11(3):345–359
Zhou CT, Xie HP, Zhu JB (2023) A dynamic strength criterion of rock materials based on energy theory. Chin J Rock Mech Eng 42(8):1890–1898
Zuo JP, Song HQ (2022) Energy evolution law and differential energy instability Model of coal-rock combined body. J China Coal Soc 47(8):3037–3051